Regular Article

New observation of nanoscale interfacial evolution in micro Cu–Al wire bonds by in-situ high resolution TEM study

Hui Xu [a,*], Ivy Qin [a], Horst Clauberg [a], Bob Chylak [a], Viola L. Acoff [b]

[a] Kulicke and Soffa Industries Inc., Fort Washington, PA 19034, United States.
[b] Department of Metallurgical and Materials Engineering, The University of Alabama, Tuscaloosa, AL 35487, United States

ARTICLE INFO

ABSTRACT

Three types of interfacial nanostructure are identified in as-bonded Cu–Al bonds: (1) Cu/~5 nm amorphous alumina layer/Al; (2) Cu/~20 nm $CuAl_2$ intermetallic particle/Al; and (3) Cu/Al. During annealing, in the areas of latter two types where alumina layer is fragmented, Cu_9Al_4 and CuAl form as second and third intermetallic layers, and grow vertically and fast together with initial $CuAl_2$. In the area of first type where alumina layer is present, $CuAl_2$ grows laterally and slowly via Cu diffusion through intermetallic compounds in the neighboring area where alumina is broken to reach Al. Cu–Al interdiffusion is dominated by Cu diffusion.

© 2015 Elsevier Ltd. All rights reserved.

Wire bonding is a key technique for electrical interconnection between integrated circuit chips and external circuitry in microelectronics. In recent years, transition from Au wire to Cu wire bonding on Al metallization pads has brought significant cost reduction [1,2]. A full understanding of Cu–Al interfacial structure and its evaluation under bonding and reliability test is of importance. Intermetallic formation at the Cu–Al wire bond improves strength. Five alloys ($CuAl_2(\theta)$, CuAl (η_2), Cu_4Al_3 (ζ_2), Cu_3Al_2 (δ) and Cu_9Al_4 (γ_2)) are possible, but excessive growth will degrade mechanical integrity. Although there have been a variety of studies on Cu–Al intermetallic compound (IMC) growth [3–13], including our previous work on intermetallic formation using Transmission Electron Microscopy (TEM) [8–10], there is no report on how the as-bonded interfacial nanostructures affect the interfacial evolution during annealing. In this letter, we take the advantage of in-situ high resolution (HR) TEM of focused ion beam (FIB) thinned specimens, to ascertain nanostructural interfacial evolution during both bonding and isothermal annealing, and especially the effect of as-bonded interfacial nanostructures on intermetallic growth, direction and phase transformation during annealing.

Thermosonic wire bonding was performed on a Kulicke and Soffa (K&S) IConn[PS] ProCu automatic ball bonder using 20 µm Cu wire and K&S BGA devices with aluminum (Al-0.5%Cu) pads of ~1 µm thick. The bonding temperature was 175 °C and bonding time 30 ms. Both electrical flame off (EFO) and bonding parameters were optimized. Forming gas (95%N_2 + 5%H_2) was used to prevent Cu oxidization at ball

formation area and bonding area at a flow rate of 0.5 L/min. TEM specimens were prepared by dual beam focused ion beam (FEI Quanta 3D 200 FIB), and its specific location is shown in the inserted image on the top left corner of Fig. 1a. Annealing was performed inside the TEM chamber, and the evolution of nano-scale interfacial structure at the bond interface was in-situ recorded (FEI F20 system at 200 kV). Fast Fourier transformation (FFT) of lattice images calculated using ImageJ 1.42q was employed to identify the IMCs. A nanoprobe beam was used for composition analysis using energy dispersive X-ray spectrometry (EDX) in high angle annular dark field (HAADF) − scanning (S)TEM mode.

Cu–Al interfaces in the as-bonded state consist of three types of morphologies, labeled as A, B and C in Fig. 1a, with details shown in Fig. 1b–d respectively. In morphology type I (Fig. 1b), a uniform amorphous layer with a thickness of approximately 5 nm is present between the crystalline copper ball and the aluminum pad. STEM–EDX suggests that such amorphous layer is alumina, which is believed to be the native aluminum oxide layer on the surface of Al pad. The alumina layer behaves as a diffusion barrier, so no intermetallic compound is formed at those areas. In morphology type II (Fig. 1c), the amorphous alumina was replaced with island-like particles of ~20 nm thick. FFT analysis of the interference lattices is consistent with $CuAl_2$ (I4/mcm, a = 0.607 nm and c = 0.488 nm) aligned along [210] orientation forming a boundary with Al (Fm-3m, a = 0.406 nm) and Cu (Fm-3m, a = 0.361 nm) in [101] (Fig. 1e and f). The morphology types I and II are consistent with our previous TEM results [8]. However, here in this study, detailed HRTEM study reveals a third distinct morphology (Fig. 1d) which corresponds to the area where Cu is directly connected with Al.

* Corresponding author.
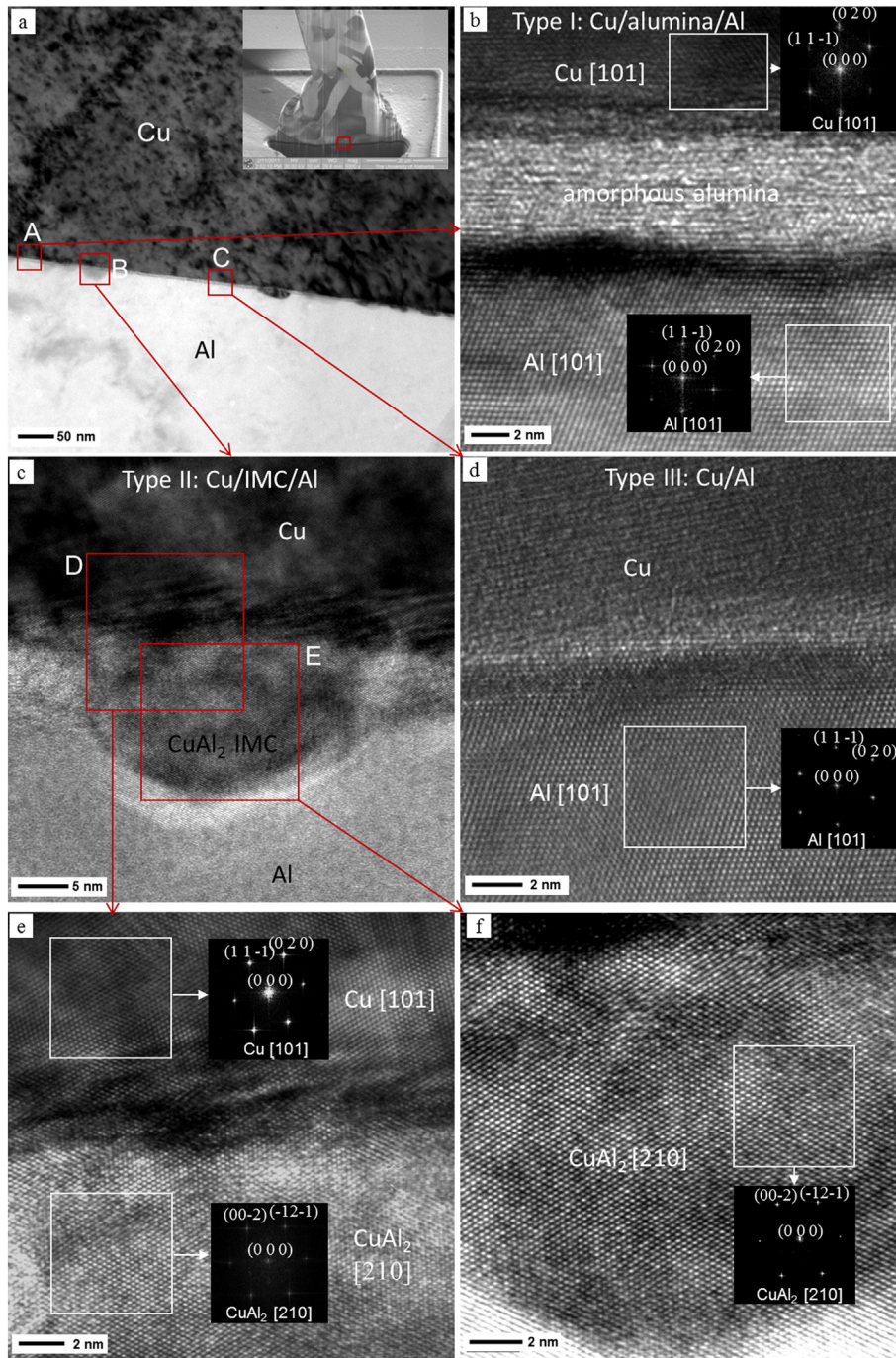E-mail address: huixu@kns.com (H. Xu).

Fig. 1. (a) Bright Field (BF) TEM showing the interface of an as-bonded Cu–Al wire bond, consisting of three types of morphologies; (b) Morphology type I: Cu/~5-nm-thick amorphous alumina/Al; (c) morphology type II: Cu/~20-nm-thick $CuAl_2$ particle/Al; (d) morphology type III: Cu directly connects Al; (e) and (f) lattice images and Fourier reconstructed patterns of region D and E in (c) with $CuAl_2$ [2 1 0].

Such connection is distinct as compared to the first two morphologies, because there is no uniform oxide layer or IMCs involved.

The 5-nm-thick native oxide layer on Al pads has significant effect on the wire-bond quality, and the formation of IMCs during the bonding process must overcome this relatively inert thin oxide layer. For these Al surface areas where the aluminum oxide is not broken, IMC could not form, and corresponds to morphology type I. For those areas where aluminum oxide is broken during bonding, IMC will form and represents morphology type II. When aluminum oxide is fragmented at the end of wire bonding stage, there is no time for Cu and Al interdiffusion to form IMC, so Cu–Al direct contact is seen, as shown in morphology type III. The degree of fragmentation of the aluminum oxide layer is

dependent on bonding parameters, bonding wire and Al pad properties. All three types of morphologies are gap and void free, but it is believed that the bonding strength of type I (Cu/alumina/Al) is weaker than type II (Cu/$CuAl_2$/Al) and type III (Cu/Al). In the next section, we will show that the IMC growth in the area of types II and III is much faster than in the area of type I. In mass production, the Cu–Al IMC coverage specification is usually more than 80% after baking for 4 h at 175 °C.

The TEM sample of Cu–Al micro-bond was heated inside a TEM chamber, so IMC growth and phase transformation was in-situ recorded, as shown in Fig. 2. IMCs grow rapidly at the early stage of annealing at 300 °C in the area of types II and III where alumina layer is fragmented during bonding. As seen in Fig. 2b, IMC thickness increases from ~20 nm